JSHC
Japan Society of Histochemistry and Cytochemistry
Established 1959

Acta Histochem. Cytochem. 57 (3): 101–108, 2024
doi: 10.1267/ahc.24-00002

Regular Article

Immunohistochemical Study of Human Mitochondrial Ferritin in the Substantia Nigra Following Subarachnoid Hemorrhage

Shogo Takahata[1], Tomoko Kato[1,2], Daijiro Yanagisawa[3], Haruka Tsubaki[1], Zulzikry Hafiz Abu Bakar[1,4], Ken-ichi Mukaisho[5], Yasushi Itoh[6,7] and Ikuo Tooyama[1]

[1]Medical Innovation Research Center, Shiga University of Medical Science, Shiga, Japan, [2]National Hospital Organization Tottori Medical Center, Tottori, Japan, [3]Molecular Neuroscience Research Center, Shiga University of Medical Science, Shiga, Japan, [4]Systems Biology Ireland, University College Dublin, Belfield, Ireland, [5]Education Center for Medicine and Nursing, Shiga University of Medical Science, Shiga, Japan, [6]Department of Pathology, Shiga University of Medical Science, Shiga, Japan and [7]Central Research Laboratory, Shiga University of Medical Science, Shiga, Japan

Received January 4, 2024; accepted March 21, 2024; published online May 10, 2024

Mitochondrial ferritin (FtMt) is a novel ferritin that sequesters iron and plays a protective role against oxidative stress. FtMt shares a high homology with H-ferritin but is expressed only in the brain, heart, and testis. In the midbrain, FtMt expression is observed in the substantia nigra. FtMt plays a neuroprotective role in the pathology of neurodegenerative diseases such as Parkinson's disease, where excessive iron induces oxidative stress, causing cell death. Herein, we investigated FtMt immunoreactivity in the brains of patients with subarachnoid hemorrhage (SAH). Double immunofluorescence labeling of tyrosine hydroxylase (TH) and FtMt showed high colocalization in the substantia nigra pars compacta (SNc) in control and SAH cases. However, in SAH cases, FtMt immunoreactivity was observed in some TH-negative neurons. Double immunofluorescence labeling of glial cell markers and FtMt showed no apparent colocalization. The number and ratio of FtMt-positive but TH-negative neurons significantly differed between the control and SAH groups. Prussian blue staining in SAH cases showed positive iron staining over a wide surface range and the substantia nigra. Thus, FtMt may be related to iron dynamics in the substantia nigra following subarachnoid hemorrhage.

Key words: immunohistochemistry, iron, mitochondrial ferritin, subarachnoid hemorrhage

I. Introduction

Subarachnoid hemorrhage (SAH) is a type of stroke that has high mortality rates and is a serious medical emergency disease [13]. In 2019, there were 12.2 million incident cases of stroke [7]. SAH accounts for approximately 5%–10% of all stroke cases, including ischemia and intracerebral hemorrhage [19]. The causes of SAH are aneurysm rupture, trauma, and genetic factors such as arteriovenous malformation and MoyaMoya disease [13, 16], with the major cause being aneurysm rupture, accounting for 80% of cases, [19] and is the most frequent and critical trigger for SAH. The cause of cerebral aneurysms is not fully understood but is considered to be related to factors such as head trauma, hypertension, atherosclerosis, and smoking [5, 11]. The common sites and frequencies of cerebral aneurysms are the middle cerebral, anterior communicating, basilar, and internal carotid arteries (37%, 25%, 22%, and 8%, respectively) [22].

Once an aneurysm ruptures, the hemorrhage elevates the intracranial pressure to produce global ischemia and hypoxia, which causes brain tissue damage and neurological dysfunction [12]. In addition, neurotoxins and iron released from the hematoma contribute to neuronal cell

Correspondence to: Ikuo Tooyama, Director and Vice president, Shiga University of Medical Science, Seta Tsukinowa-cho, Otsu 520–2192, Japan. E-mail: kinchan@belle.shiga-med.ac.jp

Table 1. *Clinical and pathological data*

Cases	Age	Sex	Postmortem delay (hr)	Pathlogical diagnosis	Vascular lesion	Iron accumulation
Control-1	60	M	5	Pancreatic cancer	ND	−
Control-2	83	F	6.5	Malignant lymphoma	ND	−
Control-3	52	M	10	Malignant lymphoma	ND	−
Control-4	47	F	3.2	Breast cancer	ND	−
Control-5	75	M	2	Esophagus cancer	ND	−
Control-6	62	M	3.3	Lung cancer	ND	−
SAH-1	64	M	12.2	Subarachnoid hemorrhage	Acom, BA	+
SAH-2	86	F	13.8	Subarachnoid hemorrhage	BA	−
SAH-3	80	F	4.6	Subarachnoid hemorrhage	BA	+
SAH-4	74	F	3.3	Subarachnoid hemorrhage	Rt.MCA	−

ND: Not detected. BA: basilar artery. Acom: anterior communicating artery. Rt.MCA: right middle cerebral artery.

death [14]. Oxidative stress induced by excessive iron overload causes brain damage after intracerebral hemorrhage [25]. Free iron (Fe^{2+}) generates oxidative stress through the Fenton reaction ($Fe^{2+} + H_2O_2 \rightarrow Fe^{3+} + \bullet OH + OH^-$) and via ferroptosis, an iron-dependent cell death pathway [3, 18]. However, sequestering of iron in ferritin protects the cell from increasing concentrations of Fe^{2+} and thereby limits oxidative cell damage [3].

Mitochondrial ferritin (FtMt) is a type of ferritin that is encoded by an intron-lacking gene on chromosome 5q23.1 [15]. The primary role of FtMt is to sequester iron and provide protection against oxidative stress [9]. Human FtMt shares approximately 79% homology in overlapping coding sequences with human H-chain ferritin, which is ubiquitously present in the cytoplasm, with a particularly high abundance in the liver and spleen [10, 15, 26], whereas FtMt expression is limited to specific tissues, namely the brain, heart, and testis [20]. Within the brain, FtMt expression is specifically observed in the substantia nigra and ventral tegmental area in the midbrain, as well as in the locus coeruleus in the pons [28]. FtMt has been shown to play a crucial neuroprotective role in the pathology of neurodegenerative diseases such as Parkinson's disease [21, 23, 27]. An elevated iron concentration was found in the substantia nigra in patients with Parkinson's disease via both postmortem histological analysis and magnetic resonance imaging [2, 6]. Notably, FtMt expression is increased under oxidative stress conditions *in vitro*, enabling protection against oxidative stress and suppression of α-synuclein expression [9]. Herein, we performed immunohistochemistry to examine FtMt expression in the substantia nigra of control and SAH cases.

II. Materials and Methods

Human brain tissue samples

This study was approved by the Ethics Committee of Shiga University of Medical Science (approval number; 2023-059). Postmortem midbrain tissues were obtained from patients with SAH (n = 4) and controls (n = 6) without any neurological diseases. Tissue collection was performed with the consent of the patients or their families. Tissues were fixed in formalin and embedded in paraffin and were then cut into 5-μm sections. The clinical and pathological information is described in Table 1.

Immunohistochemistry

Sections were deparaffinized three times in 100% xylene, followed by rehydration in 100% ethanol three times, 90% ethanol once, and 70% ethanol once. Sections were washed in running tap water, rinsed in distilled water, and then washed in 0.1 M phosphate-buffered saline (pH 7.4) containing 0.3% Triton X-100 (PBST). To block endogenous peroxidase activity, sections were incubated in 1% hydrogen peroxide solution for 20 min without agitation. After washing in PBST, antigen retrieval was performed by microwaving in 1 mM ethylenediaminetetraacetic acid (EDTA) for 4 min. Subsequently, sections were washed in PBST and blocked with 2% bovine serum albumin (BSA) in PBST for 30 min and then incubated overnight at 4°C with mouse monoclonal anti-human FtMt antibody (C65-2; IgM isotype; 0.1 μg/mL) [28] with gentle shaking. After washing in PBST, the sections were then incubated with biotinylated anti-mouse IgM antibody (1:500, Vector Laboratories, Burlingame, CA) for 1 hr at room temperature. Following another PBST wash, sections were incubated with the avidin–biotin–peroxidase complex (Vectastatin ABC Elite kit, 1:3,000, Vector Laboratories). And subsequently developed in a solution containing 0.02% 3,3-diamine-benzidine tetrahydrochloride (DAB) and 0.3% nickel ammonium sulfate in 50 mM Tris-HCl (pH 7.6) with 0.005% hydrogen peroxide for 10 min. Finally, sections were dehydrated once in 70% ethanol, once in 90% ethanol, and three times in 100% ethanol, followed by three dips in xylene. Digital images were captured using an Olympus BX50 light microscope.

Double-fluorescence immunohistochemistry

After deparaffinization and washing in PBST, antigen retrieval was performed by microwaving in 1 mM EDTA for 4 min. Subsequently, sections were washed in PBST three times and then blocked with 2% BSA in PBST for

30 min. Sections were incubated overnight with C65-2 antibody (2 μg/mL) and rabbit polyclonal antibodies against tyrosine hydroxylase (TH; 1:500, Abcam, Cambridge, UK), GFAP (1:1000, Abcam), or Iba1 (1:500, Wako Pure Chemical Industries, Osaka, Japan) at 4°C. After washing in PBST, sections were incubated for 1 hr with Alexa Fluor 568-labeled donkey antimouse IgG (1:500, Invitrogen, Frederick, MD, USA) for FtMt and Alexa Fluor 488-labeled donkey antirabbit IgG (1:500, Invitrogen) for TH, GFAP, and Iba1. Following a wash in 0.1 M PBS, sections were incubated with DAPI (Nacalai-Tesque, Kyoto, Japan) for 15 min. After another wash in PBS, sections were incubated for 50 sec with TrueBlack solution (1:40 diluted with 70% ethanol, Biotium, Fremont, CA, USA) to reduce background fluorescence. Finally, after washing in PBS, sections were cover-slipped using mounting medium (Life Technologies, Carlsbad, CA, USA). Digital images were acquired using a Leica TCS SP8 confocal laser scanning microscope (Wetzlar, Germany).

Absorption test

Absorption tests were performed to evaluate an in-house FtMt antibody C65-2. Sections were deparaffinized in xylene and ethanol as described above. After washing in PBST, sections were incubated in 1% hydrogen peroxide solution for 20 min. After washing, antigen retrieval was performed by microwaving with 1 mM EDTA for 4 min. Following a wash in PBST, sections were blocked with 2% BSA in PBST for 30 min. Sections were then incubated with preabsorbed C65-2 antibody mixed with FtMt peptide (C65-2: FtMt peptide = 1:1000, preincubation was performed overnight at 4°C) overnight at 4°C. The subsequent immunohistochemistry steps were the same as those described above.

Quantitative analysis of FtMt immunoreactivity in neurons of substantia nigra pars compacta

Quantitative analysis was performed to measure the number of FtMt-positive and TH-positive neurons and compare them between the control and SAH cases. Immunofluorescence images measuring 550 μm in length 550 μm in width were obtained using Leica SP8 confocal microscope. For quantitative analysis, total number of immunoreactive cells was counted in three immunofluorescence images that were positioned equally in the SNc. The results (cells/mm^2) were calculated by dividing total number of immunoreactive cells by total image area (0.908 mm^2). The number of FtMt-positive and -negative neurons was determined using open-source software ImageJ. Statistical analysis was conducted using GraphPad Prism version 10 software (GraphPad Software, La Jolla, CA, USA). Data were analyzed using an unpaired t-test, and significant differences were determined by a p-value < 0.05. Data are presented as mean ± SEM.

Prussian blue staining

After deparaffinization, sections were incubated for 5 min with a solution containing equal volumes of potassium ferrocyanide solution and hydrochloric acid solution of an Iron Stain Kit (ScyTek Laboratories, West Logan, Utah, USA). Sections were rinsed thoroughly in distilled water and stained in Nuclear Fast Red Solution for 5 min. After rinsing four times in distilled water, sections were dehydrated three times in 100% ethanol for 2 min each, followed by three dips in xylene.

III. Results

Characterization of mouse monoclonal anti-human FtMt antibody

Previously, we developed a mouse monoclonal anti-human FtMt antibody, C65-2 [28]. Herein, we conducted an absorption test on SAH cases to verify the specificity of this antibody. Without preincubation with FtMt peptides, FtMt immunoreactivity using C65-2 was detected as purple puncta, with neuromelanin (NM) appearing as brown granules (Fig. 1). Conversely, when C65-2 was preincubated with FtMt peptides, no immunoreactivity was observed. Thus, the antibody specifically recognizes and binds to FtMt.

Localization of FtMt immunoreactivity in the substantia nigra of SAH

Immunohistochemistry in the midbrain sections of control and SAH cases was performed to investigate the changes in FtMt immunoreactivity in SAH. In the control cases, FtMt immunoreactivity was predominantly observed in NM-containing neurons, with varying staining densities across different areas (Fig. 2A). In SAH cases, although FtMt immunoreactivity was also primarily observed in NM-containing neurons, FtMt immunoreactivity was in some NM-free neurons (Fig. 2B).

Colocalization of FtMt and TH immunoreactivity in the substantia nigra

We performed double immunofluorescence labeling to investigate the colocalization of TH and FtMt in the substantia nigra. TH immunoreactivity was prominently observed in the substantia nigra pars compacta (SNc) in the control and SAH cases (Fig. 3A, D), and FtMt immunoreactivity was highly colocalized with TH immunoreactivity (Fig. 3C, F). In the control cases, several small red particles were present in the TH-negative area, but this may be considered nonspecific staining (Fig. 3C, arrowheads). In the SAH cases, several notable FtMt-immunoreactive aggregates were observed in TH-negative areas (Fig. 3F, arrows).

Localization of FtMt and glial cell markers

To test whether FtMt is present in astrocytes and microglia, we performed double immunofluorescence staining for FtMt and glial cell markers, GFAP and Iba1. No

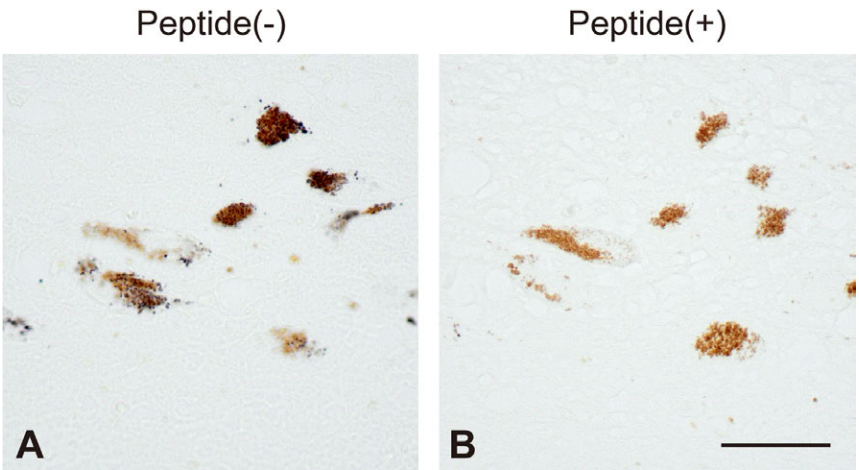

Fig. 1. Absorption test for mitochondrial ferritin (FtMt) antibody in the substantia nigra pars compacta of an SAH case. **A**: Without preincubation of FtMt peptide, FtMt was stained dark purple in SAH-1. **B**: With preincubation of FtMt peptide, no dark purple pigments were apparent in the section. Neuromelanin was observed as light brown pigments. Bar = 20 μm.

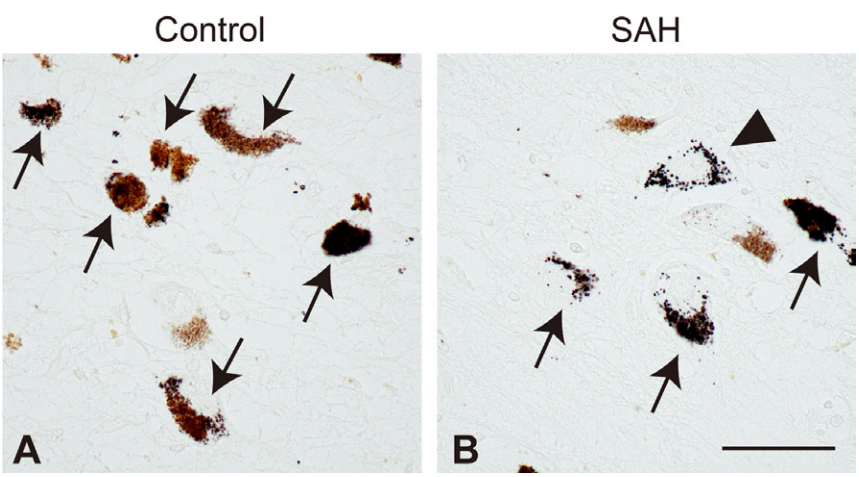

Fig. 2. Changes in the localization of mitochondrial ferritin (FtMt) in the substantia nigra pars compacta of SAH. Representative photomicrographs of FtMt immunoreactivity in midbrain sections of a control (**A**) and an SAH case (**B**). Positive-stained areas correspond with neuromelanin-positive cells (arrows). Conversely, limited immunoreactivity was observed in neuromelanin-negative cells (arrowhead). Bar = 20 μm.

apparent colocalization of FtMt was present with glial cell markers in SAH cases (Fig. 4). Therefore, FtMt expression in SAH is primarily limited to neurons.

FtMt immunoreactivity in TH-positive and -negative neurons

To compare FtMt expression in TH-positive and -negative neurons between control and SAH cases, we statistically analyzed the amount of immunoreactivity. The number of TH-positive neurons did not significantly differ between the control and SAH cases (Fig. 5A). Meanwhile, the number of FtMt-positive neurons was significantly higher in SAH cases than in control cases (Fig. 5B). The number of double-positive neurons for both FtMt and TH in the SNc did not significantly differ (Fig. 5C). Similarly, the percentage of double-positive neurons for FtMt and TH among total TH-immunoreactive neurons did not significantly differ (Fig. 5D). The number of FtMt-positive and TH-negative neurons was significantly higher in SAH cases than in control cases (Fig. 5E). Furthermore, the percentage of FtMt-positive and TH-negative neurons among total FtMt-immunoreactive neurons was significantly increased in SAH cases compared with that in control cases (Fig. 5F).

Iron localization in SAH cases

We performed Prussian blue staining to detect iron in the midbrain sections of patients with SAH. No staining was present in control cases, even in the perivascular areas. Conversely, two out of four SAH cases showed blue pigmentation along with a hemorrhage over the surface of the brain below the arachnoid mater (Fig. 6A). Iron was

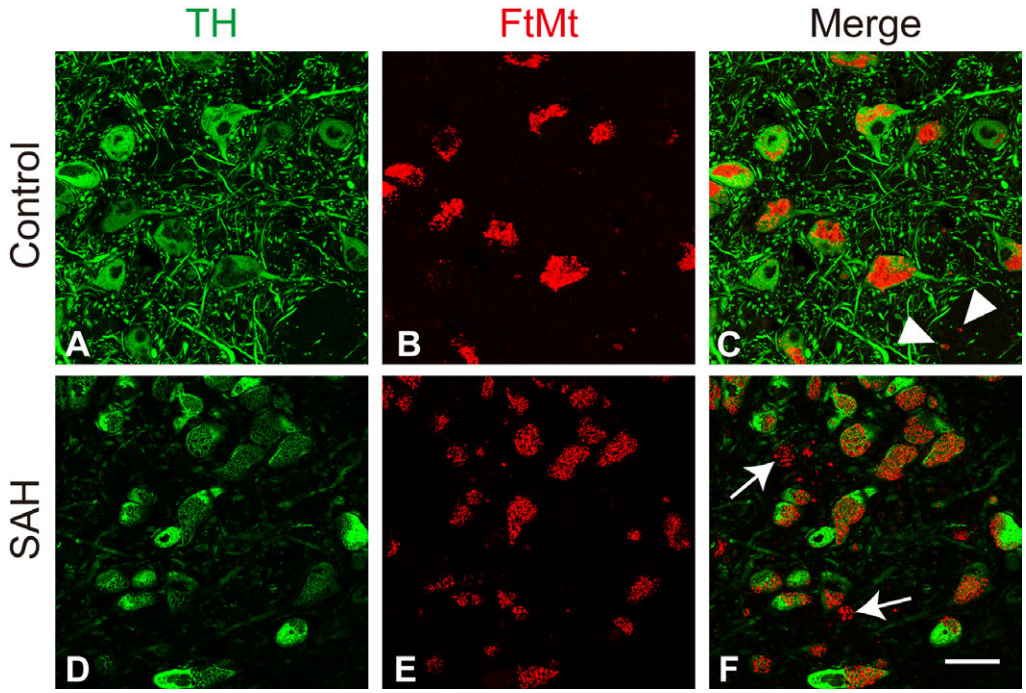

Fig. 3. Mitochondrial ferritin (FtMt) was detected in dopaminergic neurons and other structures. Representative immunofluorescence images for tyrosine hydroxylase (TH) (**A**, **D**) and FtMt (**B**, **E**) in the substantia nigra pars compacta in the control case (**A**–**C**) and the patient with subarachnoid hemorrhage (**D**–**F**). Merged images are shown in (**C**) and (**F**). A few small red particles are present in the TH-negative area in the control cases (arrowheads). Most of the FtMt immunoreactivity was observed in TH-positive cells, whereas FtMt immunoreactivity was also found in some cells that were not immunopositive for TH in SAH cases (arrows). Bar = 50 μm.

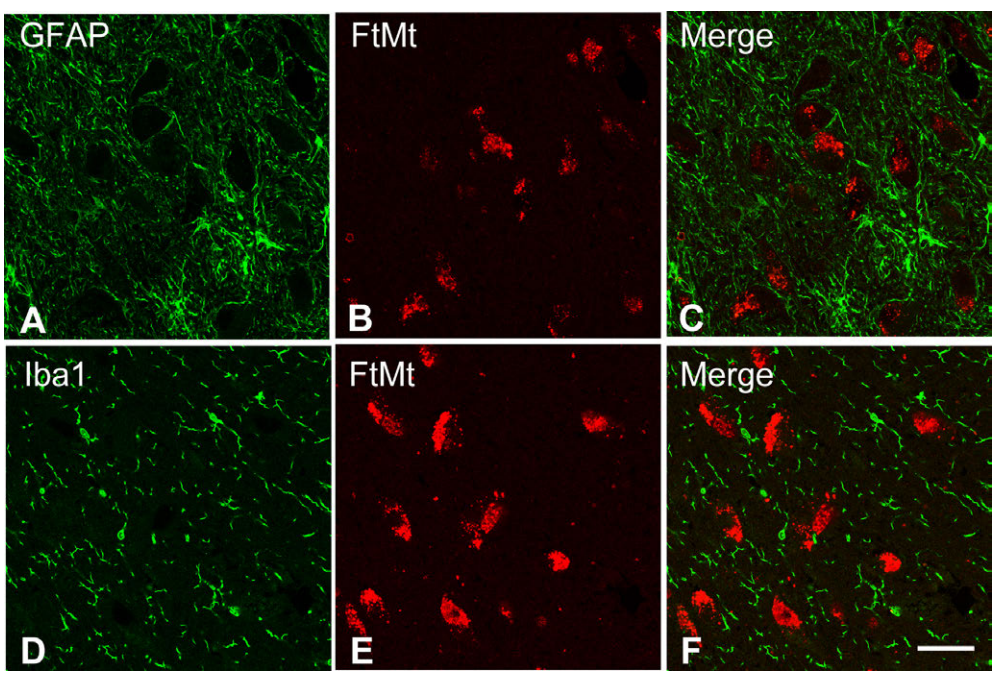

Fig. 4. Mitochondrial ferritin (FtMt) was not detected in astrocytes or microglia in patients with a subarachnoid hemorrhage (SAH-1). Representative immunofluorescence images for GFAP (**A**), Iba1 (**D**), and FtMt (**B**, **E**) with SAH cases. Merged images were shown in (**C**) and (**F**). FtMt immunoreactivity did not colocalize with GFAP or Iba1. Bar = 50 μm.

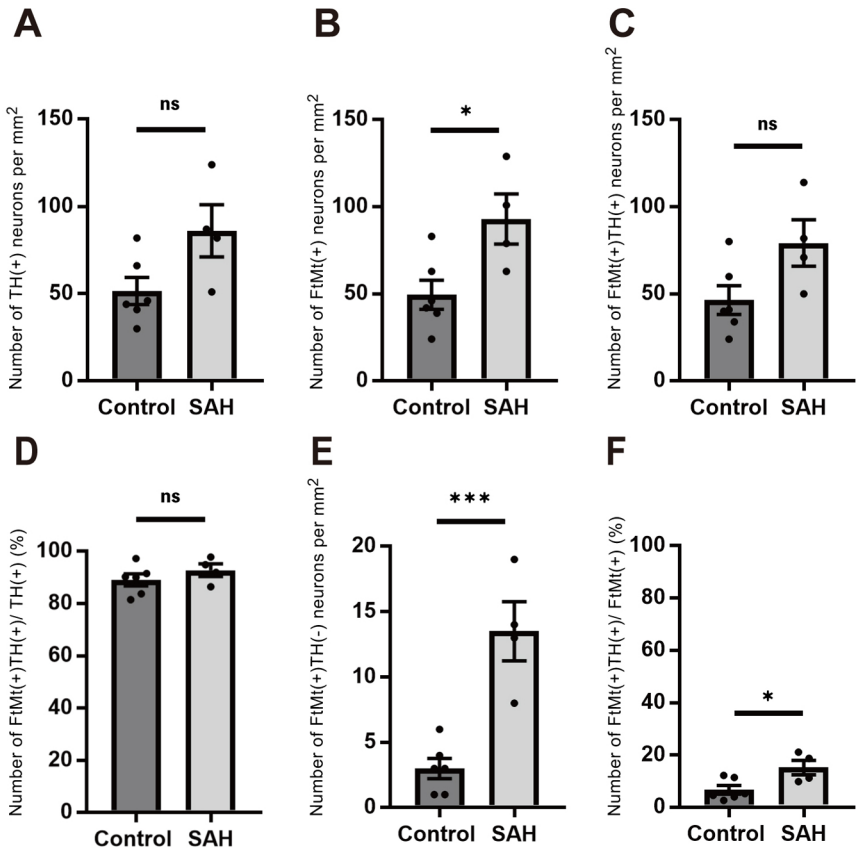

Fig. 5. Quantitative analysis of mitochondrial ferritin (FtMt) and tyrosine hydroxylase (TH) in the substantia nigra pars compacta (SNc) from controls (n = 6) and patients with SAH (n = 4). **A**: Number of positive neurons for TH in the SNc ($p = 0.0540$). **B**: Number of positive neurons for FtMt in the SNc ($p = 0.0227$). **C**: Number of double-positive neurons for FtMt and TH in the SNc ($p = 0.0570$). **D**: Percentage of double-positive neurons for FtMt and TH to total TH-immunoreactive neurons in the SNc ($p = 0.3140$). **E**: Number of FtMt-positive and TH-negative neurons in the SNc ($p = 0.0008$). **F**: Percentage of FtMt-positive and TH-negative neurons to total FtMt-immunoreactive neurons in the SNc ($p = 0.0221$). Data are presented as the mean ± SEM. *$p < 0.05$, ***$p < 0.001$ (unpaired t-test).

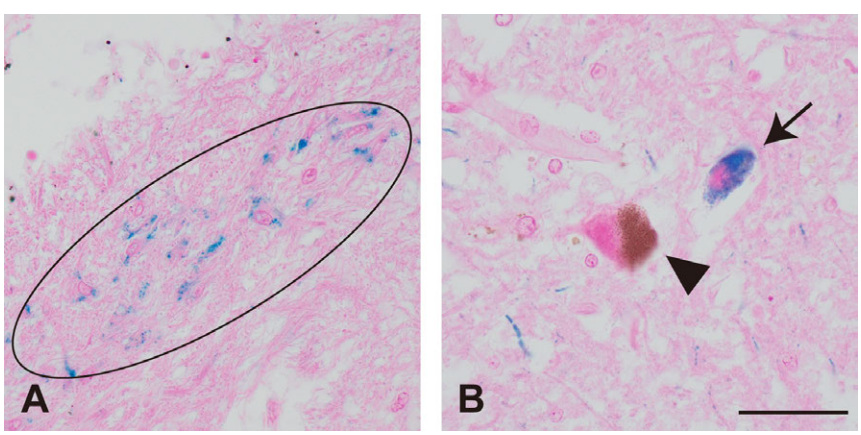

Fig. 6. Iron accumulation in patient with a subarachnoid hemorrhage. Representative photomicrographs of Prussian blue staining for iron detection. (**A**) Positive staining shown by blue color along with a hemorrhage over the surface of the brain below the arachnoid mater (oval). (**B**) Positive staining in intracellular neural cell in the substantia nigra pars compacta (arrow). Neuromelanin was observed as a dark brown pigments but did not colocalize with iron (arrowhead). Bar = 20 μm.

observed in the extracellular space and in the cell body in the SNc (Fig. 6B).

IV. Discussion

Herein, we investigated the localization of FtMt in dopaminergic neurons, astrocytes and microglia, using their respective markers, TH, GFAP, and Iba-1, respectively, in the SNc of patients with SAH. FtMt immunoreactivity in patients with SAH was detected in TH-positive dopaminergic neurons but not in astrocytes or microglia. Furthermore, several FtMt-positive puncta were observed in TH-negative neurons in SAH cases. Similarly, a degree of FtMt immunoreactivity was observed in NM-free neurons. This result is consistent with a previous study on progressive supranuclear palsy cases [1]. Two reasons are considered for this observation. The probable reason is that FtMt expression is induced in TH-negative neurons in the SNc in SAH cases. In the substantia nigra, most neuron types are dopaminergic neurons [17, 30]. Thus, TH-negative neurons are considered as neurons that have lost TH expression prior to the onset of SAH.

NM is recognized as accumulating high amounts of iron in the SNc [29, 30]. In addition, cellular ferritin is a potent iron sequester. However, the large amount of iron released in SAH may exceed the binding capacity of NM and the sequestering capacity of cellular ferritin. Consequently, FtMt expression is induced in TH-negative neurons to sequester excess iron in SAH.

The possible reason is that iron overload might temporarily impair TH expression in neurons. TH requires catalytic nonheme ferrous iron as a cofactor [8]. Ferrous iron overload can produce increased levels of ferric iron and oxidative stress through the Fenton reaction and subsequently decreases the level of ferrous iron and inhibits TH activity. This can reduce the synthesis of neurotransmitters such as dopamine. Therefore, in SAH, a high content of Fe^{2+} can cause acute damage that may temporarily prevent TH expression.

In two SAH cases in this study, iron staining was positive in the SNc, which is consistent with results in a previous report, which indicated Prussian blue-stained iron within hemorrhages in 8 of 12 cases [4]. Herein, staining was observed along with a hemorrhage over the surface of the brain. Furthermore, the presence of staining does not depend on patient conditions, such as the duration between symptom onset and surgery, which is also consistent with a previous study [4]. In one case, positive iron staining was widely observed in the substantia nigra. Iron may have some influence on dopaminergic neurons and FtMt. Additionally, an NM-free neuron contains a large deposit of iron, suggesting that iron is absorbed in TH-negative neurons. FtMt leads free iron to the cell body to sequesters this [9]. Thus, an increasing number of FtMt-positive but TH-negative neurons are present in SAH, and may subsequently react with free iron and absorb this through FtMt. Therefore, investigating other stroke patterns, such as intracranial hemorrhage and ischemic infarction, may be of value as these cause more direct damage to brain lesions, and FtMt levels have been shown to be upregulated in the ischemic brains of mice [24].

This study has some limitations. For instance, we primarily relied on qualitative immunohistochemical staining of human sections, rather than on quantitative methods such as western blot analysis. The sections were already fixed in formalin after the autopsy, so it was not appropriate to perform this analysis.

In summary, we found that FtMt immunoreactivity increased in TH-negative neurons in SAH cases. Iron-positive staining was observed in 50% of the SAH cases, one of which showed positive staining in the substantia nigra, but was not evident in any control cases. Further study is needed to identify the relationship between FtMt, cellular ferritin, and iron in SAH pathology using a quantitative approach.

V. Conflicts of Interest

Shogo Takahata is the CEO of Medpreneur, a university-based venture company.

VI. Acknowledgments

This study was supported by a Grant-in-Aid for Scientific Research from the Japan Society for the Promotion of Science (Grant Numbers 20K20588, I.T.). We are sincerely grateful to Mr. T. Yamamoto of the Central Research Laboratory, Shiga University of Medical Science, for technical support with microscopy.

VII. References

1. Abu Bakar, Z. H., Kato, T., Yanagisawa, D., Bellier, J. P., Mukaisho, K. I. and Tooyama, I. (2021) Immunohistochemical study of mitochondrial ferritin in the midbrain of patients with progressive supranuclear palsy. *Acta Histochem. Cytochem.* 54; 97–104.
2. Bartzokis, G., Cummings, J. L., Markham, C. H., Marmarelis, P. Z., Treciokas, L. J., Tishler, T. A., *et al.* (1999) MRI evaluation of brain iron in earlier- and later-onset Parkinson's disease and normal subjects. *Magn. Reson. Imaging* 17; 213–222.
3. Cao, Y., Li, Y., He, C., Yan, F., Li, J. R., Xu, H. Z., *et al.* (2021) Selective ferroptosis inhibitor Liproxstatin-1 attenuates neurological deficits and neuroinflammation after subarachnoid hemorrhage. *Neurosci. Bull.* 37; 535–549.
4. Castellani, R. J., Mojica, G. and Perry, G. (2016) The role of the iron stain in assessing intracranial hemorrhage. *Open Neurol. J.* 10; 136–142.
5. Chiara, R., Matteo, F., Federico, D. S., Anna, L. M., Francesco, C., Enrico, C., *et al.* (2024) Epidemiology and treatment of atraumatic subarachnoid hemorrhage over 10 years in a population-based registry. *Eur. Stroke J.* 9; 200–208.
6. Dexter, D. T., Carayon, A., Javoy-Agid, F., Agid, Y., Wells, F. R., Daniel, S. E., *et al.* (1991) Alterations in the levels of iron, ferritin and other trace metals in Parkinson's disease and other

neurodegenerative diseases affecting the basal ganglia. *Brain* 114; 1953–1975.
7. Feigin, V. L. (2021) Global, regional, and national burden of stroke and its risk factors, 1990–2019: a systematic analysis for the Global Burden of Disease Study 2019. *Lancet Neurol.* 20; 795–820.
8. Flydal, M. I. and Martinez, A. (2013) Phenylalanine hydroxylase: Function, structure, and regulation. *IUBMB Life* 65; 341–349.
9. Guan, H., Yang, H., Yang, M., Yanagisawa, D., Bellier, J. P., Mori, M., *et al.* (2017) Mitochondrial ferritin protects SH-SY5Y cells against H2O2-induced oxidative stress and modulates α-synuclein expression. *Exp. Neurol.* 291; 51–61.
10. Hara, Y., Yanatori, I., Tanaka, A., Kishi, F., Lemasters, J. J., Nishina, S., *et al.* (2020) Iron loss triggers mitophagy through induction of mitochondrial ferritin. *EMBO Rep.* 21; e50202.
11. Jung, K. H. (2018) New pathophysiological considerations on cerebral aneurysms. *NeuroIntervention* 13; 73–83.
12. Kusaka, G., Ishikawa, M., Nanda, A., Granger, D. N. and Zhang, J. H. (2004) Signaling pathways for early brain injury after subarachnoid hemorrhage. *J. Cereb. Blood Flow Metab.* 24; 916–925.
13. Lawton, M. T. and Vates, G. E. (2017) Subarachnoid hemorrhage. *N. Engl. J. Med.* 377; 257–266.
14. Lee, J. Y., Keep, R. F., He, Y., Sagher, O., Hua, Y. and Xi, G. (2010) Hemoglobin and iron handling in brain after subarachnoid hemorrhage and the effect of deferoxamine on early brain injury. *J. Cereb. Blood Flow Metab.* 30; 1793–1803.
15. Levi, S., Corsi, B., Bosisio, M., Invernizzi, R., Volz, A., Sanford, D., *et al.* (2001) A human mitochondrial ferritin encoded by an intronless gene. *J. Biol. Chem.* 276; 24437–24440.
16. Li, X., Liu, C., Zhu, L., Wang, M., Liu, Y., Li, S., *et al.* (2023) The role of high-resolution magnetic resonance imaging in cerebrovascular disease: A narrative review. *Brain Sci.* 13; 677.
17. Lo Bianco, C., Ridet, J. L., Schneider, B. L., Déglon, N. and Aebischer, P. (2002) α-synucleinopathy and selective dopaminergic neuron loss in a rat lentiviral-based model of Parkinson's disease. *Proc. Natl Acad. Sci. U S A* 99; 10813–10818.
18. Peng, Y., Chang, X. and Lang, M. (2021) Iron homeostasis disorder and Alzheimer's disease. *Int. J. Mol. Sci.* 22; 12422.
19. Rincon, F., Rossenwasser, R. H. and Dumont, A. (2013) The epidemiology of admissions of nontraumatic subarachnoid hemorrhage in the United States. *Neurosurgery* 73; 217–222.
20. Santambrogio, P., Biasiotto, G., Sanvito, F., Olivieri, S., Arosio, P. and Levi, S. (2007) Mitochondrial ferritin expression in adult mouse tissues. *J. Histochem. Cytochem.* 55; 1129–1137.
21. Shi, Z. H., Nie, G., Duan, X. L., Rouault, T., Wu, W. S., Ning, B., *et al.* (2010) Neuroprotective mechanism of mitochondrial ferritin on 6-hydroxydopamine-induced dopaminergic cell damage: Implication for neuroprotection in Parkinson's disease. *Antioxid. Redox Signal* 13; 783–796.
22. Tau, N., Sadeh-Gonik, U., Aulagner, G., Turjman, F., Gory, B. and Armoiry, X. (2018) The Woven EndoBridge (WEB) for endovascular therapy of intracranial aneurysms: Update of a systematic review with meta-analysis. *Clin. Neurol. Neurosurg.* 166; 110–115.
23. Tsubaki, H., Yanagisawa, D., Kageyama, Y., Hafiz Abu Baker, Z. H., Mukaisho, K. I. and Tooyama, I. (2023) Immunohistochemical analysis of mitochondrial ferritin in the midbrain of patients with Parkinson's disease. *Acta Histochem. Cytochem.* 56; 21–27.
24. Wang, P., Cui, Y., Ren, Q., Yan, B., Zhao, Y., Yu, P., *et al.* (2021) Mitochondrial ferritin attenuates cerebral ischaemia/reperfusion injury by inhibiting ferroptosis. *Cell Death Dis.* 12; 447.
25. Xi, G., Keep, R. F. and Hoff, J. T. (2006) Mechanisms of brain injury after intracerebral hemorrhage. *Lancet Neurol.* 5; 53–63.
26. Yang, H., Yang, M., Guan, H., Liu, Z., Zhao, S., Takeuchi, S., *et al.* (2013) Mitochondrial ferritin in neurodegenerative diseases. *Neurosci. Res.* 77; 1–7.
27. Yang, M., Yang, H., Guan, H., Bellier, J. P., Zhao, S. and Tooyama, I. (2016) Mapping of mitochondrial ferritin in the brainstem of Macaca fascicularis. *Neuroscience* 328; 92–106.
28. Yang, M., Yang, H., Guan, H., Kato, T., Mukaisho, K., Sugihara, H., *et al.* (2017) Characterization of a novel monoclonal antibody against human mitochondrial ferritin and its immunohistochemical application in human and monkey substantia nigra. *Acta Histochem. Cytochem.* 50; 49–55.
29. Zecca, L., Gallorini, M., Schünemann, V., Trautwein, A. X., Gerlach, M., Riederer, P., *et al.* (2001) Iron, neuromelanin and ferritin content in the substantia nigra of normal subjects at different ages: Consequences for iron storage and neurodegenerative processes. *J. Neurochem.* 76; 1766–1773.
30. Zucca, F. A., Segura-Aguilar, J., Ferrari, E., Muñoz, P., Paris, I., Sulzer, D., *et al.* (2017) Interactions of iron, dopamine and neuromelanin pathways in brain aging and Parkinson's disease. *Prog. Neurobiol.* 155; 96–119.